

# A novel mitochondrial septin-like protein, ARTS, mediates apoptosis dependent on its P-loop motif

Sarit Larisch\*, Youngsuk Yi†, Rona Lotan\*, Hedviga Kerner\*, Sarah Eimerl, W. Tony Parks‡, Yossi Gottfried\*, Stephanie Birkey Reffey§, Mark P. de Caestecker†, David Danielpour¶, Naomi Book-Melamed‡, Rina Timberg‡, Colin S. Duckett§, Robert J. Lechleider†#, Hermann Steller\*\*, Joseph Orly‡, Seong-Jin Kim‡ and Anita B. Roberts†‡‡

\*Pathology Department, Rambam Medical Center, Haifa, Israel

†Laboratory of Cell Regulation and Carcinogenesis, and §Metabolism Branch, National Cancer Institute, National Institutes of Health, Bethesda, Maryland 20892-5055, USA

‡Department of Biological Chemistry, The Alexander Silberman Institute of Life Sciences, Hebrew University of Jerusalem, Jerusalem 91904, Israel

¶Cancer Center and Department of Pharmacology, Case Western Reserve University, 11001 Cedar Road, Cleveland, Ohio 44106, USA

#Current address: Department of Pharmacology, Uniformed Services University of the Health Sciences, 4301 Jones Bridge Road, Bethesda, Maryland 20814-4799, USA

\*\*Howard Hughes Medical Institute, Department of Biology, Massachusetts Institute of Technology, 68-430, Cambridge, Massachusetts 02139, USA

‡‡e-mail: robertsa@dce41.nci.nih.gov

**Here we describe a protein product of the human septin H5/PNUTL2/CDCrel2b gene, which we call ARTS (for apoptosis-related protein in the TGF- $\beta$  signalling pathway). ARTS is expressed in many cells and acts to enhance cell death induced by TGF- $\beta$  or, to a lesser extent, by other apoptotic agents. Unlike related septin gene products, ARTS is localized to mitochondria and translocates to the nucleus when apoptosis occurs. Mutation of the P-loop of ARTS abrogates its competence to activate caspase 3 and to induce apoptosis. Taken together, these observations expand the functional attributes of septins previously described as having roles in cytokinesis and cellular morphogenesis.**

Apoptosis is a morphologically distinct form of programmed cell death that is important in development, tissue homeostasis and a wide variety of diseases, including cancer, AIDS, stroke, myopathies and various neurodegenerative disorders<sup>1,2</sup>. A central step in apoptosis is the activation of the caspases (for cysteine aspartase), an unusual class of cysteine proteases that are widely expressed as inactive zymogens<sup>3</sup>. These caspase zymogens are converted to the active protease as cells are selected to die. Once activated, caspases are thought to cleave a variety of important structural proteins, enzymes and regulatory molecules, including nuclear lamins, proteins associated with the cytoskeleton, topoisomerase I, small nuclear ribonucleoproteins and DNase inhibitors, among others<sup>4</sup>.

A central goal of apoptosis research is to understand how activation of the caspase-based death programme is restricted to cells that are destined to die. Mitochondria have been shown to play an important role in sensing and propagating cell death signals. For example, the release of cytochrome *c* from mitochondria into the cytoplasm is thought to be a critical step for activation of the apoptotic programme<sup>5,6</sup>. Cytosolic cytochrome *c* is thought to serve as a co-factor for the activation of caspase by Apaf-1, a homologue of the *Caenorhabditis elegans* cell-death gene *ced-4* (refs 6,7). It has also been proposed that other mitochondrial constituents, such as apoptosis-inducing factor (AIF), may also participate in the induction of apoptosis<sup>8</sup>. However, much remains to be learned about the signalling pathways that are used to select specific cells for death, and how different pathways are integrated to regulate the decision between cell death and survival.

TGF- $\beta$  is a multifunctional protein with a broad spectrum of cellular activities ranging from the regulation of target gene activity to the control of cell growth and apoptosis<sup>9-11</sup>. Although some signal-transduction pathways of TGF- $\beta$  are known to be mediated by SMAD proteins<sup>12</sup> or by MAP kinase pathways<sup>13,14</sup>, very little is

known about TGF- $\beta$  apoptotic pathways. Here we report the identification of a new factor, termed ARTS, which we originally identified from its role in TGF- $\beta$ -induced apoptosis of NRP-154 rat prostate epithelial cells<sup>15</sup>. ARTS is a mitochondrial septin-like protein derived from alternative splicing of the H5/PNUTL2/hCDCrel2a/2b gene. Septins are a family of conserved proteins that have been shown to be required for cytokinesis in yeast, *Drosophila* and mammals<sup>16</sup>. It has also been suggested that they form a cytoskeletal system that may have a more general role in cellular morphogenesis, and possibly also in the assembly of signalling complexes. The previously characterized septins localize to actin-rich regions, such as the cleavage furrow of dividing cells, neuronal growth cones and the leading edge of migrating sheets of epithelial cells, but ARTS localizes to mitochondria in living cells. We show that ARTS undergoes a mitochondrial to nuclear translocation at the onset of apoptosis, and that it promotes cell death in response to TGF- $\beta$ , and to a lesser extent by the tumour-necrosis factor TNF- $\alpha$  and Fas ligand. Taken together, these observations describe a new function for this unique septin-like protein and suggest that ARTS is required for the induction of cell death mediated by TGF- $\beta$  and possibly by other apoptotic stimuli.

## Results

**Cloning and characterization of ARTS.** To search for new genes in the TGF- $\beta$  apoptotic signalling pathway, we used a retroviral insertional mutagenesis approach on NRP-154 rat prostate epithelial cells, which are extremely sensitive to TGF- $\beta$ -mediated apoptosis<sup>9</sup>. Phenotypic selection was used to isolate several clones resistant to apoptosis by TGF- $\beta$ . One clone, M-NRP1, which contained only one vector integration site and retained its complement of TGF- $\beta$  receptors and its response to TGF- $\beta$  by induction of fibronectin and plasminogen activator inhibitor-1 expression<sup>15</sup>, was chosen for

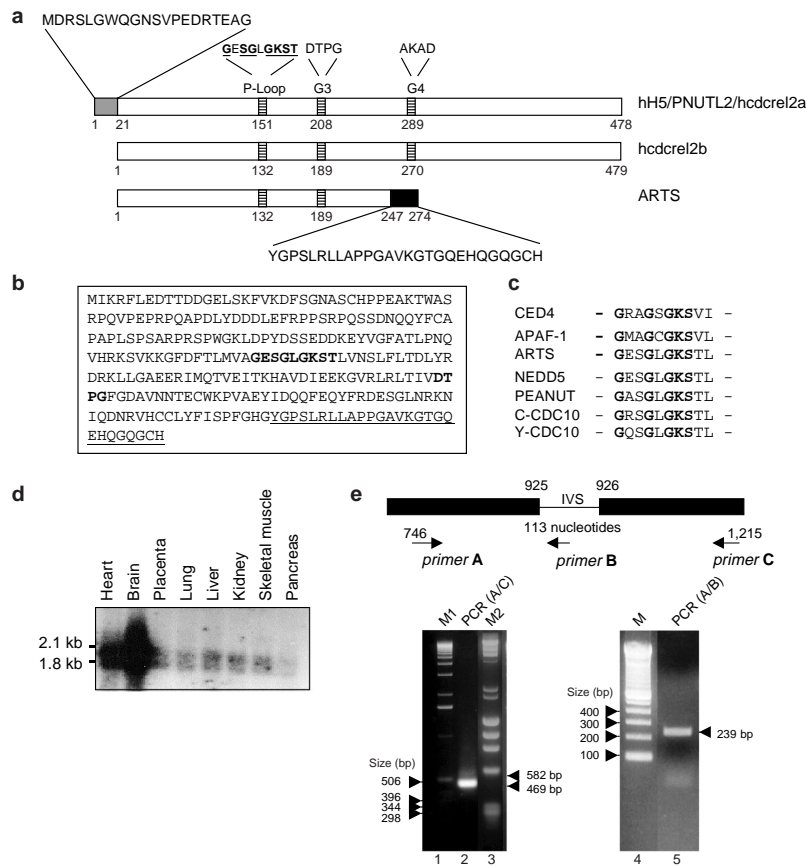


**Figure 1 ARTS represents a unique transcript of the H5 septin gene.** **a**, Alignment of the sequences encoding hH5/PNUTL2/hcdcrel2a, hcdcrel2b and ARTS showing the conserved G1, G3 and G4 motifs and the unique 27-amino-acid C terminus of ARTS. **b**, Complete amino-acid sequence of ARTS. P-loop and G3 motifs are bold, and the unique C terminus is underlined. **c**, Alignment of the P-loop domains of the apoptogenic proteins CED-4 and Apaf-1 and septin-family members human ARTS and NEDD5, *Drosophila* Peanut, *C. elegans* C-CDC10, and Y-CDC10 from the yeast *Saccharomyces cerevisiae*. **d**, Northern-blot analysis of a multiple human tissue blot

probed with ARTS cDNA. **e**, Top, schematic representation of a portion of the H5 gene showing the flanking exons and the intervening sequence (IVS) of 113 nucleotides found only in ARTS mRNA. The numbers are from the published human H5 cDNA sequence (Genbank accession no. AF035811). PCR using human fetal brain cDNA and primer sets A and C showed the 469-bp H5- and 582-bp ARTS-specific fragments (lane 2); primer sets A and B detected only the 239-bp ARTS-specific fragment (lane 5). Molecular markers used are 1-kb ladder (M1, lane 1),  $\lambda$ Hind III/ $\phi$ X174 RF DNA/HaeIII fragments (M2, lane 3), and 100-bp ladder (M, lane 4).

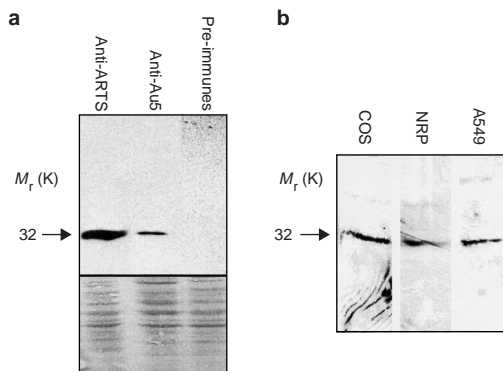


**Figure 2 ARTS is detected as a 32K protein in cell lysates.** **a**, Western blots of lysates of COS cells transfected with ARTS-AU5 and blotted with anti-ARTS, raised to the 27-amino-acid unique C terminus of ARTS, anti-AU5, or pre-immune serum. Loading control shows staining with Ponceau S (Sigma). **b**, Endogenous ARTS was detected using the anti-ARTS antibody in COS, NRP-154 and A549 cells as a 32K band. No other bands were detected with this antibody. *M<sub>r</sub>*, relative molecular mass.

further analysis. Screening of a genomic library prepared from M-NRP1 cells, and subsequently a human fetal brain complementary DNA library with exonic sequences found in the rat genomic sequence, resulted in the isolation of a 1.8-kilobase (kb) cDNA fragment. Sequencing of the cDNA, revealed an open-reading frame (ORF) of 823 base pairs (bp) that was predicted to encode a polypeptide of 274 amino acids (Fig. 1a).

A BLAST search of Genbank using the ORF sequence showed that the molecule that we have called ARTS matches human chromosome 17q22-23 genomic sequences (GenBank accession number HRPK AC005666). It is likely to be the product of an alternatively spliced form of the hH5/PNUTL2/hCDCrel2 septin-family gene in which the 113 base pairs of intervening sequence between exons VI and VII of the H5 gene is not spliced out, generating a new in-frame stop codon<sup>17-19</sup> (Y. Yi, S. Larisch and S.-J. Kim, manuscript in preparation; Fig. 1a,b,e). As a result, ARTS shares its amino-terminal start site with hCDCrel-2b but has a unique 27-amino-acid carboxy terminus not found in any other products of this gene (Fig. 1a). Importantly, ARTS retains a phosphate-binding site (Walker A box P-loop or G1 motif; GXSGXGKST)<sup>20,21</sup>, conserved in the septin family of proteins but also found in many ATP/GTPases, including the apoptotic regulators CED-4 (refs 22,23) and Apaf-1 (ref. 5) (Fig. 1c).

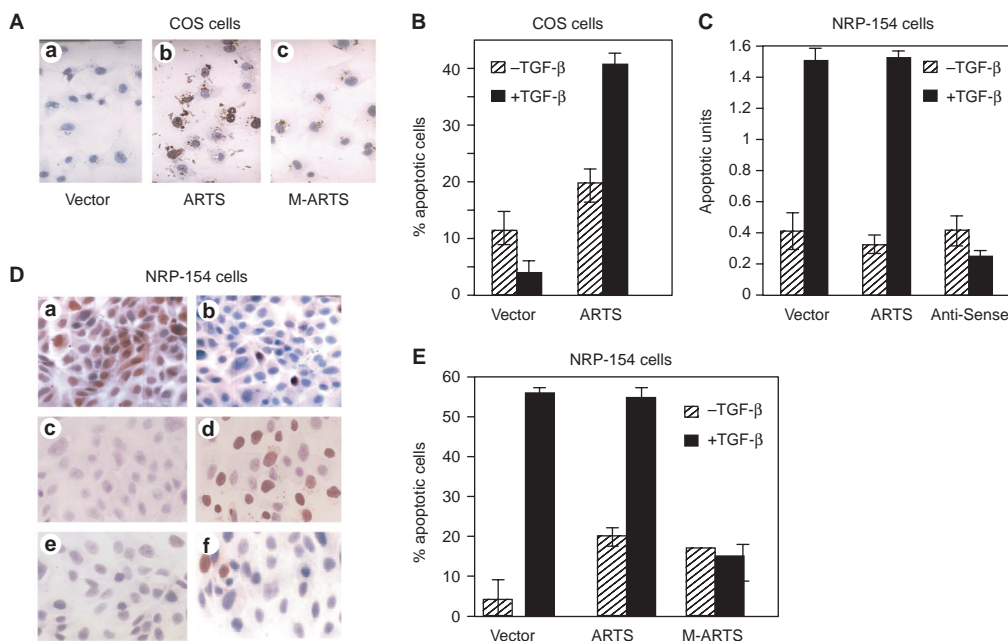


**Figure 3 ARTS is essential for TGF $\beta$ -induced apoptosis.** **A**, Apoptosis induced in COS cells was examined using a TUNEL assay on cells transfected with equal concentrations of either pcDNA3 control vector (**a**), ARTS (**b**) or M-ARTS–pcDNA3 (**c**), and treated with TGF- $\beta$  for 24 h. Apoptotic nuclei are stained red, non-apoptotic nuclei blue. Original magnification,  $\times 40$ . **B**, Immunofluorescence assay determining the percentage of transfected cells exhibiting apoptotic nuclei. COS cells were co-transfected with TGF- $\beta$  receptors and either empty AU5 vector or ARTS–AU5 and then stained with anti-AU5–fluorescein antibody and counterstained with DAPI for counting fragmented nuclei. TGF- $\beta$  treatment was for 24 h. **C**, **D**, Functional effects of antisense ARTS in NRP-154 cells were determined using both a cell death detec-

tion ELISA assay (**C**) and a TUNEL assay (**D**, **c–f**). **D**, The effect of antisense ARTS on expression of endogenous ARTS in NRP-154 cells was assessed by immunohistochemical techniques using anti-ARTS antibodies (**a**, sense, **b**, antisense; red staining). Apoptosis was assessed by TUNEL staining of cells transfected with either wild-type ARTS (**c**, **d**) or antisense ARTS (**e**, **f**) and treated with either vehicle (**c**, **e**) or TGF- $\beta$ , 10 ng ml $^{-1}$  for 24 h (**d**, **f**). Cells transfected with vector and wild-type ARTS responded similarly to TGF- $\beta$  (as shown in **C**). **E**, Ability of M-ARTS to repress TGF $\beta$ -mediated apoptosis dependent on endogenous ARTS in NRP-154 cells. Assay was as in **B**, **C**, **E**. Results expressed as mean ( $\pm$ s.e.m.) of duplicate assays, and repeated three times with similar results.

Of two other motifs (G3, DXXG and G4, XKXD) found in small GTPases and common to most other septins<sup>19</sup>, only the G3 motif is preserved in ARTS, indicating that it might not bind GTP as other septins do.

A cDNA probe detected two species of approximately 1.8 and 2.0 kb in a human multiple-tissue northern blot, demonstrating that the ARTS/H5/PNUTL2/hCDCrel2a/2b gene is expressed more highly in brain and heart than in other tested tissues examined (Fig. 1d). To confirm the existence of the unique ARTS transcript, we performed the polymerase chain reaction (PCR) on human fetal brain cDNA, using primer sets that either detect both H5 and ARTS or are specific for ARTS. PCR using primers A and C produced two fragments of 582 and 469 bp (Fig. 1e). The 469-bp fragment, lacking the intervening sequence, is the major transcript in fetal brain. Sequencing the 582-bp fragment subcloned into the TOPO cloning vector showed that it contains the intervening sequence predicted in the ARTS transcript (data not shown). To selectively detect the ARTS transcript, we used a primer set in which the 3' primer (primer B in Fig. 1e) is from the intervening sequence. This PCR produced the expected 239-bp fragment (lane 5).

Immunoprecipitation with anti-AU5 antibodies of lysates of metabolically labelled COS cells transfected with an ARTS–AU5-tagged construct showed the protein to have a relative molecular mass of about 32,000 ( $M_r$ ~32K), slightly higher than that predicted, suggesting that post-translational modifications of ARTS have occurred (data not shown). Both anti-AU5 antibodies and specific anti-ARTS peptide antibodies raised against the unique 27 C-terminal amino acids of ARTS (Fig. 1b) also react with a 32K protein in lysates of COS cells transfected with ARTS–AU5 (Fig. 2a). These anti-ARTS antibodies also detect endogenous ARTS in lysates of

COS, NRP-154 and A549 human lung carcinoma cells (Fig. 2b). In all cell lysates tested, only a single 32K band is detected with this antibody. As predicted, the related septins H5 and hCDCrel2b are not detected by the anti-ARTS antibody when overexpressed in COS cells (data not shown).

**ARTS enhances TGF- $\beta$ -dependent apoptosis and caspase activation.** To determine whether ARTS plays a role in TGF $\beta$ -induced apoptosis, an AU5 epitope-tagged ARTS expression construct was transiently transfected into various cell lines. As assessed by a TUNEL assay, COS cells transfected with control vector did not undergo apoptosis when treated with 10 ng ml $^{-1}$  TGF- $\beta$  for 24 h (Fig. 3A,a), whereas cells transfected with ARTS exhibited strong TUNEL staining after TGF- $\beta$  treatment. A mutant construct of ARTS (M-ARTS) containing three mutations in the conserved P-loop domain (GKS to ENP) failed to induce competence to undergo apoptosis in the presence of TGF- $\beta$  (Fig. 3A,c), suggesting that this motif is critical for the apoptogenic activity of ARTS. To quantify the apoptosis, COS cells transfected with AU5-tagged ARTS were identified by indirect immunofluorescence. The number of transfected cells also exhibiting apoptotic nuclear fragmentation was determined as a percentage of the total number of transfected cells (Fig. 3B). Transfection of ARTS increased both basal and TGF- $\beta$ -induced apoptosis compared with cells transfected with vector, indicating that overexpression of ARTS may shift the balance of TGF- $\beta$  signalling pathways towards apoptotic end points in certain cells such as COS (Fig. 3) and A549 (data not shown), which do not normally undergo apoptosis in response to TGF- $\beta$ .

In NRP-154 cells, which are extremely sensitive to TGF- $\beta$ -induced apoptosis<sup>9,15</sup>, transfection with ARTS does not increase TGF- $\beta$ -dependent apoptosis compared with cells transfected with

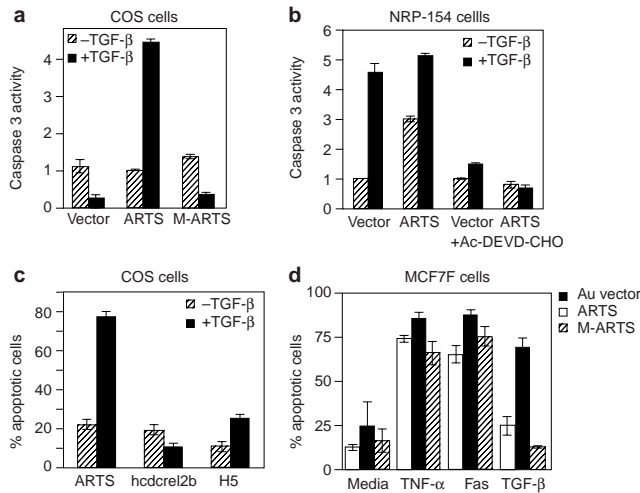


**Figure 4** ARTS-induced apoptosis correlates with caspase activation. **a, b**, Caspase 3-like activity was determined in COS cells (**a**) and NRP-154 cells (**b**). Data are standardized as changes relative to untreated vector alone. Ac-DEVD-CHO caspase 3-specific inhibitor was added. **c**, The related septins H5 and *hdcrcel2b* expressed in COS cells do not make cells competent to undergo apoptosis following treatment with TGF-β, 10 ng ml<sup>-1</sup> for 24 h. Cells staining positively for the AU5 epitope were assessed morphologically for apoptosis. **d**, MCF7 cells transfected with either wild-type ARTS or the P-loop mutant, M-ARTS, were treated with either TNF-α, anti-Fas or TGF-β for 24 h. ARTS potentiates apoptosis to each of these stimuli as assessed by counting apoptotic nuclei of GFP-positive cells. Results are mean (±s.e.m.) of duplicate (**a-c**) or triplicate (**d**) assays, and repeated three times with similar results.

vector alone, as measured by an enzyme-linked immunosorbent assay (ELISA) for quantification of internucleosomal fragmentation of DNA (Fig. 3C). To address the question whether endogenous ARTS might be essential for TGF-β-induced apoptosis, an antisense construct of ARTS was transfected into these cells. This markedly reduced the level of endogenous ARTS protein as detected with the anti-ARTS antibody and visualized by immunohistochemistry (red staining in Fig. 3D,a,b). Both the ELISA assay (Fig. 3C) and TUNEL stain (Fig. 3D,c-f) showed that NRP-154 cells transfected with antisense ARTS exhibited a marked reduction in their apoptotic response to TGF-β, indicating that expression of endogenous ARTS is necessary to direct TGF-β signalling towards apoptotic end points. In these cells, the P-loop mutant, M-ARTS, also suppressed TGF-β-dependent apoptosis (Fig. 3E). This finding implies that it might act in a dominant-negative manner to block the activity of endogenous ARTS, as has been suggested for a P-loop mutant of the septin CDCrel-1 (refs 16,24).

Caspase 3, a key player in programmed cell death, is activated by a proteolytic cascade in cells undergoing apoptosis<sup>3,4</sup>. To investigate whether ARTS-dependent apoptosis induced by TGF-β involves effector caspases, we assayed caspase 3 activation in COS and NRP-154 cells. In COS cells, overexpression of ARTS caused a marked increase in the activation of caspase 3 following treatment with TGF-β (Fig. 4a), consistent with the requirement for exogenous ARTS to increase TGF-β-dependent apoptosis in these cells (Fig. 3A,B). Similar data were obtained in A549 cells (data not shown). In contrast, in NRP-154 cells, which are intrinsically sensitive to TGFβ-induced apoptosis<sup>9</sup>, caspase 3 was activated by treatment with TGF-β, and overexpression of ARTS had little effect (Fig. 4b), similar to its lack of effect on TGF-β-induced apoptosis (Fig. 3C). Treatment with the caspase 3 aldehyde inhibitor Ac-DEVD-CHO inhibited TGF-β-induced caspase activity in all cells examined (Fig. 4b). These results suggest that, similar to the requirement for

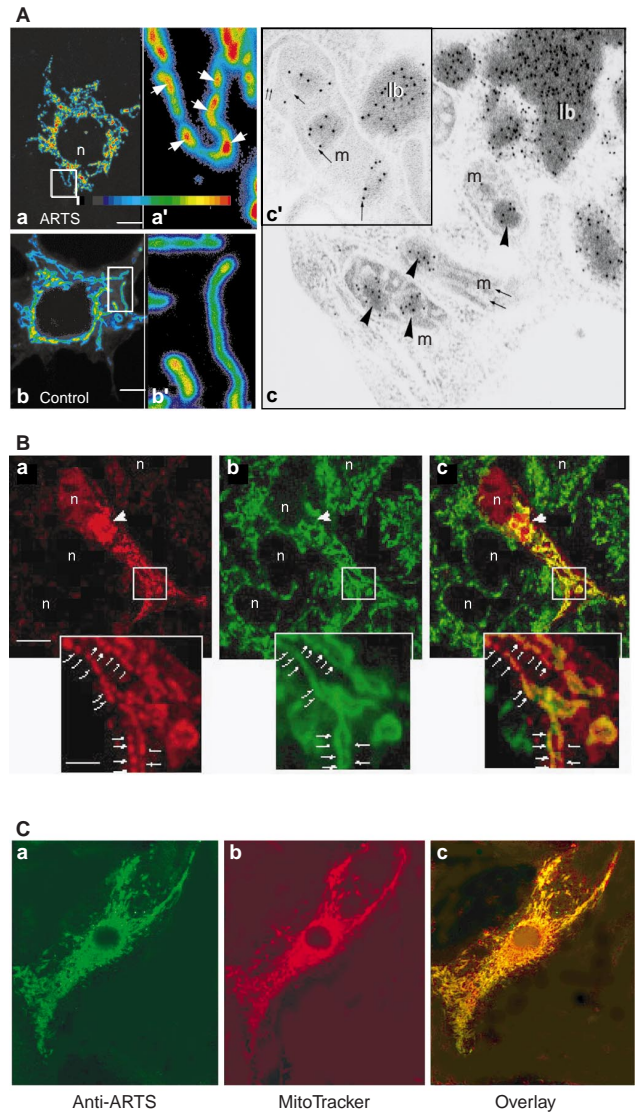


**Figure 5** ARTS localizes to mitochondria. **A**, Intracellular localization of ARTS-AU5 depicted by confocal (**a, a'**) and electron microscopy (**c, c'**) in transfected COS cells. **a**, Pseudocolour image of fluorescence intensities shows punctuate staining of ARTS-AU5 specifically localized in the mitochondria (arrows in **a'**); a high-power scan of the boxed in area in **a**. **b**, Control transfection with a typical mitochondrial protein, steroidogenic acute regulatory protein, StAR28 (ref. 32), shows a homogeneous distribution of StAR in the mitochondria distinct from that of ARTS (**b'**, high-power image of the boxed area in **b**); n, nucleus. Scale bars, 10 μm. **c, c'**, Immuno-gold electron microscopy of ARTS-AU5-transfected COS cells demonstrates distinct localization of ARTS in mitochondria (m) and electron-dense lysosomal-like bodies (lb). Mitochondrial ARTS is concentrated in discrete areas of electron-dense mitochondrial matrix (arrowheads in **c**) delineated by inner-membrane spaces (arrows in **c'**). Magnification, ×61,000. **B**, Confocal analysis of double-immunofluorescence staining of transfected COS cells showing the localization of ARTS-AU5 (**a**, red), cytochrome c (**b**, green), or both (**c**, overlay). Insets, higher magnification of the boxed areas. Note the extensive overlap in the distribution of ARTS and cytochrome c. Consistent with the electron microscopy data, the pattern of mitochondrial ARTS is punctate (arrows in **a** and **c**, insets) compared with the more continuous pattern of cytochrome c in mitochondria (arrows in **b**, inset). Unlike cytochrome c, ARTS is also present in perinuclear aggregates that presumably correspond to lysosomal-like bodies (arrowheads, see also **A,c**). **C**, Endogenous ARTS localizes to mitochondria of primary rat neonatal cardiomyocytes. Co-localization (yellow) of endogenous ARTS as stained by anti-ARTS (green) and MitoTracker (red), as visualized by confocal fluorescence microscopy (magnification ×270). Scale bars represent 10 μm (**A, B**) and 2.5 μm (insets).

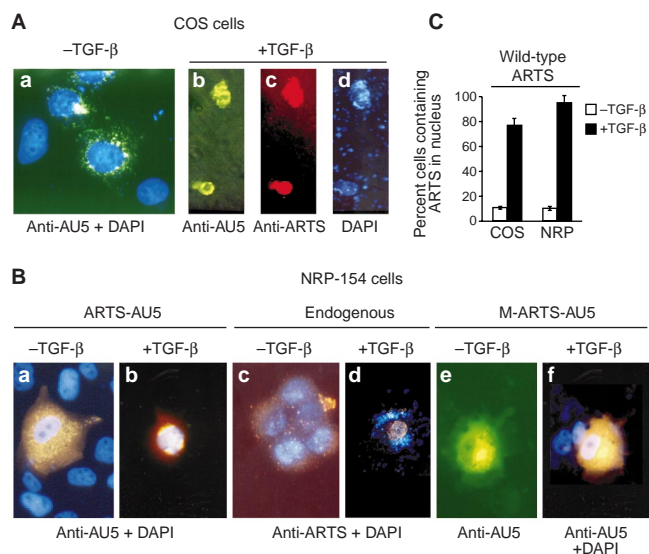


**Figure 6** Ligand-dependent translocation of ARTS from the mitochondria to the nucleus during apoptosis as shown by fluorescence microscopy. **A, a–d**, FITC-conjugated secondary antibodies reacting with anti-AU5-tagged ARTS (green) in transfected COS cells (**a, b**); Rhodamine-conjugated secondary antibodies reacting with anti-ARTS antibodies detected both endogenous and exogenous expression of ARTS as red staining (**c**). Nuclei were visualized with DAPI (**a, d**). After TGF- $\beta$  treatment, ARTS translocates to the nucleus coincident with nuclear fragmentation as seen with DAPI stain (**d**). **B**, NRP-154 cells transfected with ARTS-AU5 (**a, b**) or M-ARTS mutated in its P-loop motif (**e, f**) and non-transfected cells (**c, d**) were stained as described in **A**. Both transfected and endogenous ARTS shows a punctate pattern in NRP-154 cells (**a, c**) and translocates to the nucleus after TGF- $\beta$  treatment, concomitant with nuclear degradation (**b, d**);  $\times 100$ . M-ARTS (green) has a subcellular distribution distinct from that of wild-type ARTS (**e, f**). The pattern of M-ARTS staining does not change when TGF- $\beta$  is added (not shown);  $\times 100$ . **C**, The percentage of transfected cells exhibiting nuclear staining of ARTS was determined in COS and NRP-154 cells. The addition of TGF- $\beta$  caused an 8- to 9-fold increase in the number of cells containing ARTS in their nuclei.

caspsases in TGF- $\beta$ -dependent apoptosis in FaO cells<sup>25</sup>, ARTS is likely to use previously described apoptotic pathways to activate caspase 3-like effector cysteine proteases to kill cells.

Transient transfection of the related septins H5 and hCDCrel2b into COS cells did not induce competence to undergo TGF- $\beta$ -dependent apoptosis, demonstrating that this activity was unique to ARTS (Fig. 4c). Similar results were obtained using human breast carcinoma MCF7F cells (data not shown), which stably express the Fas receptor<sup>26,27</sup>.

To investigate whether the effects of ARTS on apoptosis are restricted to pathways downstream of TGF- $\beta$ , we transfected ARTS or its P-loop mutant into MCF7Fas cells<sup>26,27</sup>. In these cells, wild-type but not mutant ARTS strongly potentiated apoptosis induced by TGF- $\beta$ , but only weakly increased the already substantial degree of apoptosis induced by TNF- $\alpha$  and an anti-Fas/Apo1 agonistic antibody (Fig. 4d). SMAD pathways and MAP kinase pathways have both been implicated in the mediation of apoptosis by TGF- $\beta$ <sup>28–31</sup>. Future studies will address whether either of these pathways is important in ARTS-mediated apoptosis of TGF- $\beta$  or whether ARTS functions downstream of different stimulus-dependent pathways that initiate the apoptotic cascade.

**ARTS undergoes a TGF- $\beta$ -dependent mitochondrial-to-nuclear translocation.** To determine the subcellular localization of ARTS, we performed confocal microscopic analysis using anti-AU5 antibodies in COS cells transfected with an ARTS-AU5-tagged construct. This

revealed a particulate pattern of staining (Fig. 5A,a,a') that is very similar to the distribution of the mitochondrial protein StAR28 (ref. 32), suggesting that ARTS localizes to mitochondria (Fig. 5A,b,b'). Further examination by immunoelectron microscopy (Fig. 5A,c,c') showed that ARTS was indeed localized to mitochondria and appeared to be clustered in protein-rich areas. Comparison of the subcellular distribution of transiently expressed AU5-ARTS (Fig. 5B,a) and cytochrome *c* (Fig. 5B,b) revealed extensive overlap (Fig. 5B,c) as did staining by confocal fluorescence microscopy for endogenous ARTS and a mitochondrion-specific fluorescent probe, MitoTracker (Fig. 5c). Taken together, these observations establish that ARTS is predominantly localized in mitochondria.

After TGF- $\beta$  treatment, ARTS translocates to the nucleus, both in COS (Fig. 6A, a–d, C) and NRP-154 cells (Fig. 6B, a–d, C), coincident with nuclear fragmentation. Unlike ARTS, the localization of M-ARTS does not change after treatment of cells with TGF- $\beta$  (Fig. 6B, e, f). Moreover, consistent with effects seen using apoptotic markers, nuclei of cells transfected with M-ARTS remain intact. Along with the observation that TGF- $\beta$  treatment of COS cells does not alter the nuclear and cytoplasmic localization of the related apoptotically inactive septins H5 or hCDCrel2b, respectively (data not shown), these data suggest that the mitochondrial to nuclear translocation of ARTS may be essential for its apoptogenic activity.

## Discussion

Here we describe the identification and functional characterization of ARTS, a septin-like protein product of the human H5/PNUTL2/CDCrel2b gene. ARTS localizes to mitochondria in cells but translocates to the nucleus in response to pro-apoptotic stimuli. It has previously been reported that the release of pro-apoptotic factors such as cytochrome *c* and AIF from the mitochondrial intermembrane space is critical for apoptosis<sup>6,8</sup>. Another mitochondrial protein, Smac/DIABLO, has recently been described that can induce caspase activation and apoptosis by interacting with and inactivating the apoptotic inhibitor XIAP<sup>33–35</sup>. The mitochondrial localization of ARTS and its mitochondrial-to-nuclear translocation during apoptosis suggest that ARTS may represent yet another mitochondrial factor important in the regulation of caspase activation and cell death. Whether the same apoptotic stimuli that cause opening of the mitochondrial permeability transition pore<sup>36</sup> also induce the P-loop-dependent release of ARTS from the mitochondria, or whether mitochondrial processing of ARTS is required for its release from mitochondria, are important questions that remain to be addressed.

ARTS is the first member of the septin family shown to localize to mitochondria or to play a role in apoptosis. This family of filament-forming proteins was originally found to be required for the completion of cytokinesis in diverse organisms<sup>16</sup>. The study of mammalian septins indicates that they might also be important for a variety of other cellular processes, such as membrane transport and fusion<sup>24</sup>, generation of cell polarity, or as a transient scaffold for recruiting and targeting other proteins, including elements of signal-transduction pathways (the product of the H5 gene and ARTS share a highly conserved P-loop motif). Mutation of this motif in ARTS blocks not only the effects of TGF- $\beta$  on its nuclear translocation, but also its apoptogenic activity. Likewise, analogous mutations in the mammalian septins Nedd5 and CDCrel-1 disrupt their ability to form filamentous structures and alter their cytosolic distribution<sup>24,37</sup>. This motif is therefore essential both for the apoptogenic function of ARTS and for the distinct functions of other septins. The same P-loop consensus sequence is also found in the pro-apoptotic proteins Apaf-1 (ref. 5) and its *C. elegans* homologue CED-4, where it is also critical to their apoptogenic function<sup>22</sup>. However, it is not clear whether ARTS activates caspases in a similar way to these proteins or by a different mechanism. It will be important to determine the role of ARTS in the nucleus, and to identify functionally relevant interacting proteins.

It has been proposed that components of the apoptotic machinery arose from several ancient domains recruited from proteins that performed other functions in unicellular organisms<sup>23</sup>. Our data lead us to speculate that although the ancestral role of septins may have been in cytokinesis, new septin-like proteins, such as ARTS, which are products of the same genes, may have arisen later in evolution to regulate apoptosis. Preliminary data obtained from the fruitfly *Drosophila* demonstrate that the dosage of the *peanut* gene, which encodes an ARTS homologue, is rate limiting for cell death by the pro-apoptotic genes *reaper*, *head involution defective* (*hid*) and *grim* (refs 38,39; L. Goyal, S. Larisch and H. Steller, unpublished results). These data indicate that *peanut*/ARTS might have a very general and broad apoptotic function conserved in evolution from flies to human. The finding that transcripts of septin genes are used for both cytokinesis and apoptosis points to a possible mechanistic linkage between these two cellular processes. Although it has previously been proposed that cell division and cell death may be regulated by common cellular components<sup>40</sup>, there has been little direct evidence to support this notion. Determination of the mechanism by which ARTS induces apoptosis may advance our understanding of elements common to these two phenomena. □

## Methods

### Mammalian cell culture and mutagenesis.

Insertionally mutagenized M-NRP1 cells, resistant to TGF- $\beta$ -induced apoptosis, were cloned from the parental NRP-154 cells as described<sup>15</sup>. A DNA fragment containing retroviral vector sequences was obtained from a genomic library of M-NRP1 cells and used to identify an exonic sequence. Several human cDNA libraries were screened with this sequence, which was found to hybridize most strongly to a human fetal brain cDNA library. Screening of this cDNA library using the Gene Trapper kit (Gibco) with a 20-bp primer corresponding to the rat exonic sequence resulted in isolation of 1.8-kb cDNA fragment found to contain the complete ORF of ARTS.

Cells were transiently transfected using Lipofectamine (Gibco BRL Life Technologies) or FuGENE 6 (Roche) according to the manufacturer's protocol. After 24 h, medium was replaced with 1% FBS-containing medium, with or without TGF- $\beta$  for a further 24 h. The AU5-tag expression vector was used to tag ARTS at its N terminus. Luciferase activity was determined in the cell lysate using an assay kit (Analytic Luminescence Laboratory), and a Dynatech Laboratories ML3000 luminometer. Activities were normalized on the basis of  $\beta$ -galactosidase expression from pSV-galactosidase. Experiments were repeated three times with similar results. Cell lysates were prepared from confluent cultures with and without treatment with TGF- $\beta$ 1 (10 ng ml<sup>-1</sup>) for 24 h. Protein concentrations were determined using the Bio-Rad protein assay kit, and equal amounts (50  $\mu$ g) of total cellular protein were loaded on 4–20% gradient gels (Novex), followed by electrophoretic transfer to nitrocellulose membranes (Micon Separations). Rabbit anti-ARTS (custom antibody, Sigma Israel) and mouse anti-AU5 (Babco) were used at concentration of 2.5–5  $\mu$ g ml<sup>-1</sup>. Immune complexes were detected using the enhanced chemiluminescence detection system (Pierce) with a secondary antibody coupled to horseradish peroxidase followed by autoradiography.

### PCR detection and mutagenesis of ARTS.

PCR was used to detect the H5 and ARTS transcripts using Marathon-ready cDNA from human fetal brain, PCR (Clontech) and specific primer sets for human H5 and ARTS: H5, primer A, TGTGGACACACCAGG; primer C, ACCCCGAATCGCCGCC; ARTS, primer A (as before); primer B, TCTTG-GCCTGTCCCTTGAC. (Primer B starts 59 nucleotides from the 5' end of the intervening sequence).

Point mutations in the P-loop domain were introduced using two complementary oligonucleotides encompassing this region and the QuikChange site-directed mutagenesis kit (Stratagene). One of the oligonucleotides is 5'-GGAGAGTCTGGCCTGGAGAAATCCACACTTGTCAATAGCC-3' (changed nucleotides are underlined).

### Apoptosis assays.

Detection of apoptotic cells was done using several methods. For detection of apoptosis using the TUNEL assay, cells were fixed and stained using the In Situ Cell Death Detection POD kit (Roche) and developed with Aminoethyl Carbazole (AEC) substrate solution (ZYMED). Slides were analysed using a fluorescence microscope provis AX70 (Olympus). The Cell death detection ELISA Plus kit (Roche), which detects internucleosomal fragmentation of DNA, and the Caspase 3 activity assay (Pharmingen) were used with lysates of transfected cells, according to the manufacturers' protocols. Results were read using a FL-600 microplate fluorescence reader (Bio-Tek). Quantification of apoptotic cells and immunolocalization of ARTS was performed using immunofluorescence detection; cells were blocked with 5% BSA in PBS for 30 min, then incubated with the indicated antibodies, followed by secondary antibodies conjugated with either fluorescein or rhodamine. After washes, a drop of DAPI-containing mounting solution (Vector) was added to each slide. Confocal images were obtained using confocal microscopes (Bio-Rad MRC-1024 scanhead attached to a Zeiss Axiovert 135M or Zeiss LSM510). Immunoelectron microscopy was performed as described<sup>32</sup>.

### Colocalization of MitoTracker and endogenous ARTS in mitochondria.

Neonatal rat ventricular myocytes were isolated from rats 1–2 days old, as described<sup>41</sup>. When the cells reached confluence, the medium was removed and pre-warmed (37 °C) F10 medium containing 50 nM MitoTracker RedCMXRos (Molecular Probes) was added and incubated with the cells for 30 min. Cells were washed twice with PBS, fixed and stained with anti-ARTS, as described earlier in immunofluorescence detection.

RECEIVED 15 MAY; REVISED 11 AUGUST; ACCEPTED 29 AUGUST;  
PUBLISHED 14 NOVEMBER 2000

1. Thompson, C. B. Apoptosis in the pathogenesis and treatment of disease. *Science* **267**, 1456–1462 (1995).
2. Vaux, D. L. & Korsmeyer, S. J. Cell death in development. *Cell* **96**, 245–254 (1999).
3. Nicholson, W. D. & Thornberry, N. A. Caspases: killer proteases. *Trends Biochem. Sci.* **257**, 299–306 (1997).
4. Thornberry, N. A. & Lazebnik, Y. Caspases: enemies within. *Science* **281**, 1312–1316 (1998).
5. Zou, H., Henzel, W. J., Liu, X., Lutschg, A. & Wang, X. Apaf-1, a human protein homologous to *C. elegans* CED-4, participates in cytochrome *c*-dependent activation of caspase-3. *Cell* **90**, 405–413 (1997).
6. Liu, X., Zou, H., Slaughter, C. & Wang, X. DFF, a heterodimeric protein that functions downstream of caspase-3 to trigger DNA fragmentation during apoptosis. *Cell* **89**, 175–184 (1997).
7. Li, P. *et al.* Cytochrome *c* and dATP-dependent formation of Apaf-1/caspase-9 complex initiates an apoptotic protease cascade. *Cell* **91**, 479–489 (1997).
8. Susin, S. A. *et al.* Molecular characterization of mitochondrial apoptosis-inducing factor. *Nature* **397**, 441–446 (1999).
9. Hsing, A. Y., Kadomatsu, K., Bonham, M. J. & Danielpour, D. Regulation of apoptosis induced by transforming growth factor-beta1 in nontumorigenic rat prostatic epithelial cell lines. *Cancer Res.* **56**, 5146–5149 (1996).
10. Haufel, T., Dormann, S., Hanusch, J., Schwieger, A. & Bauer, G. Three distinct roles for TGF-beta during intercellular induction of apoptosis: a review. *Anticancer Res.* **19**, 105–111 (1999).
11. Flanders, K. C. & Roberts, A. B. Transforming growth factor- $\beta$ . *Cytokine Reference* (eds Oppenheim, J. J. *et al.*) (Academic, New York, 2000).
12. Massagué, J. & Chen, Y. G. Controlling TGF-beta signaling. *Genes Dev.* **14**, 627–644 (2000).
13. Hartsough, M. T. & Mulder, K. M. Transforming growth factor-beta signaling in epithelial cells. *Pharmacol. Ther.* **75**, 21–41 (1997).
14. Engel, M. E., McDonnell, M. A., Law, B. K. & Moses, H. L. Interdependent SMAD and JNK signaling in transforming growth factor-beta-mediated transcription. *J. Biol. Chem.* **274**, 37413–37420 (1999).
15. Larisch-Bloch, S. *et al.* Selective loss of the transforming growth factor-beta apoptotic signaling pathway in mutant NRP-154 rat prostatic epithelial cells. *Cell Growth Differ.* **11**, 1–10 (2000).
16. Field, C. M. & Kellogg, D. Septins: cytoskeletal polymers or signalling GTPases? *Trends Cell Biol.* **9**, 387–394 (1999).
17. Xie, H., Surka, M., Howard, J. & Trimble, W. S. Characterization of the mammalian septin H5: distinct patterns of cytoskeletal and membrane association from other septin proteins. *Cell Motil. Cytoskel.* **43**, 52–62 (1999).
18. McKie, J. M., Sutherland, H. F., Harvey, E., Kim, U. J. & Scambler, P. J. A human gene similar to *Drosophila melanogaster peanut* maps to the DiGeorge syndrome region of 22q11. *Hum. Genet.* **101**, 6–12 (1997).
19. Zieger, B., Hashimoto, Y. & Ware, J. Alternative expression of platelet glycoprotein Ib(beta) mRNA from an adjacent 5' gene with an imperfect polyadenylation signal sequence. *Clin. Invest.* **99**, 520–525 (1997).
20. Saraste, M., Sibbald, P. R. & Wittinghofer, A. The P-loop — a common motif in ATP- and GTP-binding proteins. *Trends Biochem. Sci.* **11**, 430–434 (1990).
21. Aravind, L., Dixit, V. M. & Koonin, E. V. The domains of death: evolution of the apoptosis machinery. *Trends Biochem. Sci.* **24**, 47–53 (1999).
22. Yuan, J. & Horvitz, H. R. The *Caenorhabditis elegans* cell death gene *ced-4* encodes a novel protein and is expressed during the period of extensive programmed cell death. *Development* **116**, 309–320 (1992).
23. Chaudhary, D., O'Rourke, K., Chinnaiyan, A. M. & Dixit, V. M. The death inhibitory molecules CED-9 and CED-4L use a common mechanism to inhibit the CED-3 death protease. *J. Biol. Chem.* **273**, 17708–17712 (1998).
24. Beites, C. L., Xie, H., Bowser, R. & Trimble, W. S. The septin CDCrel-1 binds syntaxin and inhibits exocytosis. *Nature Neurosci.* **2**, 434–439 (1999).
25. Choi, K. S., Lim, I. K., Brady, J. N. & Kim, S. J. ICE-like protease (caspase) is involved in transforming growth factor beta1-mediated apoptosis in FaO rat hepatoma cell line. *Hepatology* **27**, 415–421 (1998).
26. Tewari, M., Beidler, D. R. & Dixit, V. M. CrmA-inhibitable cleavage of the 70-kDa protein component of the U1 small nuclear ribonucleoprotein during Fas- and tumor necrosis factor-induced apoptosis. *J. Biol. Chem.* **270**, 18738–18741 (1995).
27. Duckett, C. S. *et al.* Human IAP-like protein regulates programmed cell death downstream of Bcl-xL and cytochrome *c*. *Mol. Cell Biol.* **18**, 608–615 (1998).
28. Atfi, A., Buisine, M., Mazars, A. & Gespach, C. Induction of apoptosis by DPC4, a transcriptional factor regulated by transforming growth factor-beta through stress-activated protein kinase/c-Jun N-terminal kinase (SAPK/JNK) signaling pathway. *J. Biol. Chem.* **272**, 24731–24734 (1997).
29. Landstrom, M. *et al.* Smad7 mediates apoptosis induced by transforming growth factor beta in prostatic carcinoma cells. *Curr. Biol.* **10**, 535–538 (2000).
30. Yanagisawa, K. *et al.* Induction of apoptosis by Smad3 and down-regulation of Smad3 expression in response to TGF-beta in human normal lung epithelial cells. *Oncogene* **17**, 1743–1747 (1998).
31. Chen, R. H., Su, Y. H., Chuang, R. L. & Chang, T. Y. Suppression of transforming growth factor-beta-induced apoptosis through a phosphatidylinositol 3-kinase/Akt-dependent pathway. *Oncogene* **17**, 1959–1968 (1998).
32. Wang, X. *et al.* Effect of truncated forms of the steroidogenic acute regulatory protein on intramitochondrial cholesterol transfer. *Endocrinology* **139**, 3903–3912 (1998).
33. Verhagen, A. M. *et al.* Identification of DIABLO, a mammalian protein that promotes apoptosis by binding to and antagonizing IAP proteins. *Cell* **102**, 43–53 (2000).
34. Du, C., Fang, M., Li, Y., Li, L. & Wang, X. Smac, a mitochondrial protein that promotes cytochrome *c*-dependent caspase activation by eliminating IAP inhibition. *Cell* **102**, 33–42 (2000).
35. Deveraux, Q. L. & Reed, J. C. IAP family proteins — suppressors of apoptosis. *Genes Dev.* **13**, 239–252 (1999).
36. Green, D. R. & Reed, J. C. Mitochondria and apoptosis. *Science* **281**, 1309–1312 (1998).
37. Kinoshita M. *et al.* Nedd5, a mammalian septin, is a novel cytoskeletal component interacting with actin-based structures. *Genes Dev.* **11**, 1535–1547 (1997).

38. Neufeld, T. P. & Rubin, G. M. The *Drosophila* peanut gene is required for cytokinesis and encodes a protein similar to yeast putative bud neck filament proteins. *Cell* **77**, 371–379 (1994).
39. McCall, K. A. & Steller, H. Facing death in the fly: genetic analysis of apoptosis in *Drosophila*. *Trends Genet.* **13**, 222–226 (1997).
40. Guo, M. & Hay, B. A. Cell proliferation and apoptosis. *Curr. Opin. Cell Biol.* **11**, 745–752 (1999).
41. Rubin, Y., Kessler-Icekson, G. & Navon, G. The effect of furosemide on calcium ion concentration in myocardial cells. *Cell Calcium* **18**, 135–139 (1995).

## ACKNOWLEDGEMENTS

We thank M. Bloch for help and encouragement; D. Barzilai and Z. Ben-Ishai for support; Y.

Ben-Neriah, A. Yaron, S. Gutkind and M. Zohar for discussions and advice; G. Yaniv and O. Binah for providing the neonatal ventricular myocytes; and N. Frumkin and A. H. Hsing for technical assistance. We thank D. B. Hales and K. H. Hales for providing the antiserum to recombinant murine StAR; the AU5-tag expression vector was provided by S. Gutkind; TGF- $\beta$  receptor constructs were provided by J. Wrana and L. Attisano; and the p3TP-Lux construct was provided by J. Massagué. This work was supported by the Erna D. Leir Foundation for Research of Degenerative Brain Diseases, the National Alliance for Research of Schizophrenia and Depression, the National Parkinson Foundation Inc., the Israel Science Foundation funded by the Israel Academy of Sciences and Humanities (J.O.), and the NIH. H.S. is an investigator of the Howard Hughes Medical Institute. Correspondence and requests for materials should be addressed to A.B.R.